Vol. 516: 209–227, 2014
doi: 10.3354/meps10975

MARINE ECOLOGY PROGRESS SERIES
Mar Ecol Prog Ser

Published December 3

Semi-annual spawning in marine scallops strengthens larval recruitment and connectivity on Georges Bank: a model study

K. T. A. Davies[1,*], W. C. Gentleman[1], C. DiBacco[2], C. L. Johnson[2]

[1]Department of Engineering Mathematics and Internetworking, Dalhousie University, 1340 Barrington St., Halifax, NS B3J 1Y9, Canada

[2]Fisheries and Oceans Canada, Bedford Institute of Oceanography, Dartmouth, NS B2Y 4A2, Canada

ABSTRACT: Sea scallops *Placopecten magellanicus* on Georges Bank in the northwest Atlantic exhibit semi-annual spawning phenology, where the autumn spawn is dominant and the spring spawn is smaller and more variable. The spring spawn is thought to contribute little to total annual larval settlement on the Bank because fecundity is lower, larval development is slower and off-Bank transport is higher during spring. We tested the hypothesis that larval settlement during spring is negligible compared to autumn by incorporating spatially and temporally explicit information about spawning and larval mortality into a coupled biological–physical larval tracking model to investigate dispersal and connectivity during each spawning period. To accomplish this, we assimilated field data on adult density-at-size and seasonal fecundity-at-size as initial conditions into the model. We discovered that larval production varied in time (spring production on the Bank is half that of autumn) and space (spawners are concentrated along the advective pathway of the along-Bank gyre). Particle settlement and connectivity was reduced, but not negligible, during spring compared to autumn due to stronger dispersal off-Bank and into uninhabitable areas during spring. When mortality was made constant in space and time, lower larval production combined with slower growth during spring resulted in a minimal contribution of the spring spawn to annual settlement. When mortality was correlated with environmental variation in time and space, the spring spawn contributed up to one-third of the total annual larval settlement between the immediate upstream–downstream connected aggregations. We conclude that the spring spawn can make a substantial contribution to total annual larval production, and that settlement on Georges Bank and should be given more attention in field studies. Larval mortality has a strong influence on settlement during spring and autumn, and future field studies should focus on quantifying space and time variation in mortality in relation to the environment.

KEY WORDS: Sea scallop · *Placopecten magellanicus* · Georges Bank · Connectivity · Larval tracking model

INTRODUCTION

Spatially separated aggregations of benthic organisms can be connected by advective transport during their pelagic larval stage, and this connectivity influences recruitment dynamics within and among aggregations (Roughgarden et al. 1988, Cowen et al. 2000). Connectivity is a complex process consisting of larval production, dispersal, settlement and post-settlement survivorship (Cowen et al. 2000, Pineda et al. 2007). Connectivity is often studied with particle-tracking models (e.g. Tremblay et al. 1994), and increasing accessibility of high resolution circulation models has facilitated considerable research into the dynamics of larval transport and the oceanographic and biological processes underlying these dynamics

*Corresponding author: kim.davies@dal.ca

(e.g. Brown et al. 2004, Paris et al. 2005, 2007, Edwards et al. 2007). Less modeling attention has been given to the influence of spawning time and location, which by initiating dispersal, can cause variation in connectivity on the same order as physical transport (Edwards et al. 2007, Pineda et al. 2007, Metaxas & Saunders 2009). Further, larval dispersal studies either do not consider larval mortality (e.g. Hare et al. 1999), consider spatially homogenous mortality (e.g. Cowen et al. 2000), or assume low mortality (e.g. Gaylord & Gaines 2000). Interactions among spawning, mortality and transport are important because the timing and location of spawning determines the landscape of predation, food and physical conditions to which larvae are exposed (Pineda et al. 2007). In this study, we focus on these interactions by incorporating spatially and temporally explicit information about spawning and larval mortality into a coupled biological–physical larval tracking model to investigate dispersal and connectivity during semi-annual spawning events in a marine invertebrate.

Sea scallops are found throughout the world's oceans, and dense aggregations supporting valuable fisheries are concentrated in the UK and western Europe (e.g. *Pecten maximus*, *P. jacobaeus, Aequipecten opercularis*), along the east coast of North America (e.g. *Placopecten magellanicus, Argopecten irradians*), around Iceland, Japan, Australia and several other countries (Brand 2006). Major fishing grounds are relatively few in number, have persisted in particular locations for long periods, and are found in areas with persistent oceanographic features (e.g. gyres) (Sinclair et al. 1985). All scallops disperse via relatively long-lived pelagic larvae, and adult population persistence near oceanographic features suggests that larval retention and exchange, which depend upon local oceanography, limit scallop population distributions (MacLeod et al. 1985, Sinclair et al. 1985, Brand 2006). Thus, considerable research has focussed on elucidating scallop larval transport processes with the goal of explaining variation in scallop populations, particularly to aid in fisheries management (e.g. Beaumont 1982, Naidu & Anderson 1984, MacLeod et al. 1985, Tremblay & Sinclair 1992, Tremblay et al. 1994, Tian et al. 2009a,b, Gilbert et al. 2010).

Georges Bank, an offshore bank in the Gulf of Maine, supports a lucrative fishery for *P. magellanicus* (Hart & Chute 2004). Three scallop aggregations on the Bank exchange larvae and are part of the same population, but are typically managed as separate stocks (Fig. 1; Tremblay et al. 1994, Hart & Chute 2004). Dispersal and connectivity of larvae among

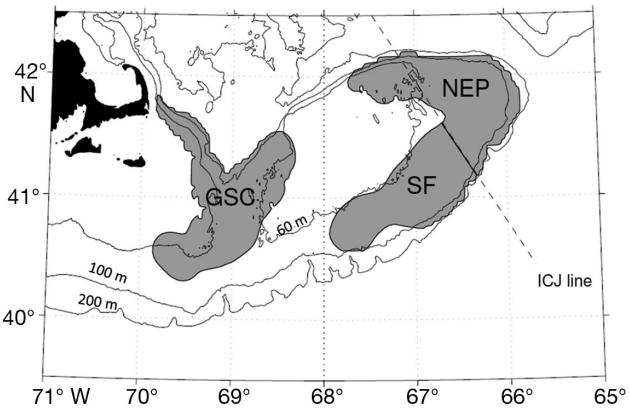

Fig. 1. Sea scallop *Placopecten magellanicus* larval tracking model domain on Georges Bank containing 3 scallop aggregations (grey): Great South Channel (GSC), Southern Flank (SF) and Northeast Peak (NEP). The International Court of Justice Line (labeled ICJ line) divides the Canadian and US exclusive economic zones. Also depicted are the 60, 100 and 200 m isobaths, and land (black) near Cape Cod

aggregations are driven by physical processes such as tidal mixing front dynamics, along-shelf currents that form a gyre circulation, and wind-induced variation in surface flows, as well as biological processes such as growth, mortality and behaviour (Tremblay et al. 1994, Tian et al. 2009a,b, Gilbert et al. 2010). The Northeast Peak (NEP) region of the Bank contains the highest abundance of adult scallops and acts as a significant larval source to other aggregations (Fig. 1; Tremblay et al. 1994). The Great South Channel (GSC) aggregation is the most retentive aggregation, receiving larvae spawned in both the NEP and Southern Flank (SF), as well as retaining locally spawned larvae (Fig. 1; Tremblay et al. 1994, Gilbert et al. 2010). In contrast, local retention of larvae spawned in the NEP and SF aggregations is negligible, and they rely mainly on input of larvae spawned in other aggregations (Tremblay et al. 1994, Tian et al. 2009a). The Georges Bank population also seeds downstream scallop beds along the New England Shelf and Mid-Atlantic Bight (Tian et al. 2009a).

Population variation in breeding cycles ranging from annual to semi-annual to continuous has been described for many scallop species (Sastry 1970, 1979, Taylor & Venn 1979, Mason 1983, Paulet et al. 1988, Brand 2006). Offshore scallop populations from Georges Bank to the Mid-Atlantic Bight exhibit a semi-annual spawning cycle (DuPaul et al. 1989, Schmitzer et al. 1991, DiBacco et al. 1995). Fecundity on Georges Bank is higher during the autumn spawn while the spring spawn is more variable, and is not detected in some years (DiBacco et al. 1995). Gilbert et al. (2010) simulated particle transport between

spring and autumn on the Bank using temperature-dependent development and found that longer pelagic duration and reduced gyre recirculation around Georges Bank during the colder spring season resulted in higher downstream particle losses than autumn. The combination of lower fecundity, reduced on-Bank retention and slower development during the colder spring season suggests that spring-spawned scallop larvae may contribute little to settlement on the Bank compared to autumn. However, 2 important processes — seasonally-varying scallop spawning production and mortality — have not been considered in previous studies of scallop larval dispersal on the Bank. Our objective is to test the hypothesis that the spring spawn makes a negligible contribution to scallop production and settlement on Georges Bank by investigating how spatial and seasonal variation in larval production, transport and mortality affect the relative contribution of spring and autumn spawned-larvae to total annual settlement.

METHODS

Characterizing aggregation- and season-specific scallop larval production

Seasonal and size-specific adult female fecundity

The densities (m^{-2}) of newly-spawned eggs within each of 3 scallop aggregations (NEP, GSC, SF) and 2 spawning seasons (spring and autumn) that comprise the initial spawning conditions in our model were estimated empirically using the product of the size-dependent seasonal-average fecundity (eggs $female^{-1}$) and local density of adult female scallops of specific size-classes on Georges Bank. Female fecundity (wet gonad weight, WGW) data were collected from stations on the NEP on a bi-weekly basis between 1984 and 2004 via Fisheries and Oceans Canada monitoring surveys or commercial vessels (DiBacco et al. 1995). The research cruise data represent intensive sampling of a 12-station grid distributed over the northeastern portion of Georges Bank (Fig. 1 in DiBacco et al. 1995); however, a rigid spatial-temporal sampling strategy was not possible due to variation in commercial fishing activity. All samples were collected using a scallop drag, from depths between 66 and 102 m.

Scallop spawning events on the Bank are generally synchronous (i.e. co-located individuals initiate spawning at similar times) over 2 to 4 wk periods in spring and autumn (DiBacco et al. 1995, Fig. S1 in the Supplement at www.int-res.com/articles/suppl/m516p209_supp.pdf). The reproductive output (fecundity) of female spawners is proportional to the magnitude of decrease in WGW (g) over a spawning period, which can be derived by measuring WGW from individuals collected before, during and after the spawning period. Here, seasonal fecundity-at-size ($f_{season,size}$, eggs $female^{-1}$ for a given size-class and season) was derived from WGW measured on 30 or more individuals per station, and several stations were sampled throughout the spawning period each year from 1984 through 2004. Field sampling and laboratory analyses presented here are an extension of the analysis described by DiBacco et al. (1995), who examined WGW collected during 1984 to 1992. We have simply extended the time series presented in that paper.

Fecundity was estimated in 3 steps: dividing scallops into size classes, measuring changes in WGW that indicated spawning events, and calculating a mean change in WGW among years within each season. Both reproductive output increases with scallop body size (Langton et al. 1987, this study), and this variation was observed in a time series of WGW divided into 3 discrete size classes (small: 50 to 95 mm; medium: 95 to 120 mm; large: 120 to 170 mm shell height). The mean WGW (±95% CI) of all individuals within each year and size class was calculated, and these statistics used to visually quantify statistically significant decreases in WGW among adjacent, bi-weekly time steps, which we considered to represent spawning events (Fig. S1). There were generally 2 significant decreases per year — one in April/May and one in August/September — although occasionally multiple spring spawns occurred within a year. When multiple spring spawns occurred, we conservatively used the average fecundity of all spring spawns, since we could not decipher whether this pattern was caused by spatial variation in the timing of gamete release among individuals at different sampling locations (in which case, the seasonal-average is appropriate), or whether a cascading synchronous spawn was measured at multiple times and locations (in which case, an integral among spawns may be more appropriate). Since many eggs may not be viable and many viable eggs may not get fertilized, our estimate represents a maximum average egg production (as in McGarvey et al. 1992). Observed intra- and inter-annual variations in the frequency and intensity of spawn will be examined in detail elsewhere. For the purposes here, the climatological average decrease in WGW over all years within each season and size class was calculated, then divided by an average egg weight of 1.6×10^{-7} g

(Langton et al. 1987) to estimate the average number of eggs released female^{-1} for a given size-class and season ($f_{size,season}$). Our resulting size-specific estimates are consistent with estimates made in autumn by McGarvey et al. (1992).

Aggregation and size-specific adult female density

The spatial distribution of adult scallop density within each aggregation was characterised using data provided by Fisheries and Oceans Canada (Smith et al. 2009) and the USA National Oceanic and Atmospheric Administration (Hart & Chute 2004, D. Hart pers. comm.) during scallop monitoring surveys that spanned the years 1994 through 2004. Adult densities were estimated from standard scallop stock assessment surveys. These surveys used a random stratified design in which the ocean was divided into zones, or strata, of similar depth and habitat, and then dredge and camera samples were taken randomly within these zones. The design of the annual surveys was based upon stratification by commercial effort. Logbooks of the commercial fleet from the preceding months were analyzed to determine levels or strata of arbitrary catch rates. Areas of high catch rates were sampled more frequently as they represent areas most important to the fleet (and presumably the areas of greatest abundance). A regular array of data points was established from which random sampling stations were chosen from each stratum. Samples were collected using a modified commercial 8-foot sea scallop dredge with a mesh liner to retain the very small seed scallops. Survey data were standardized to a tow area of 1951 m^2 tow^{-1} in Canadian and 4500 m^2 in US waters.

Adult scallop density within each size class (c_{size}, ind. km^{-2}) was estimated in each 1 km^2 grid cell within each aggregation using geostatistical analysis of scallop survey data collected within each aggregation. Aggregation borders were defined where adult density decreased below 25 km^{-2}, as in Gilbert et al. (2010). Log-transformed adult density data from all tows within each size class were kriged at 1 km^2 resolution using the geostatistical package 'geoR' (Ribeiro & Diggle 2001, www.leg.ufpr.br/geoR). Briefly, the spatial dependence between observations was identified by an anisotropic (directed along-isobath) semi-variogram that was estimated empirically using the following equation:

$$\gamma^*(h) = \frac{1}{2M(h)} \sum_{\alpha=1}^{M(h)} [p(u_\alpha + h) - p(u_\alpha)]^2 \quad (1)$$

In which: $\gamma^*(h)$ represents the semi-variance, $M(h)$ is the number of pairs of scallop density observations, u is a 2D vector of spatial coordinates, $p(u)$ is the scallop density as a function of spatial location, and h is the lag distance between pairs. In the case of anisotropy, $h = \sqrt{(h_x / a_x)^2 + (h_y / a_y)^2}$ where a_x, a_y are the ranges in the along- and cross-isobath directions. The empirical semi-variogram was then fit with an exponential model, which was used to krige the data:

$$\gamma^*(h) = C0 + C1\,[1 - \exp(-3h / a)] \text{ for } 0 < h < d \quad (2)$$

in which d is the maximum distance in which the semi-variogram is defined, $C0$ is the nugget and $C1$ is the sill. Exponential model parameters were estimated by ordinary least squares. Kriged adult density data were divided by 2 to estimate the number of females, assuming an equal sex ratio.

Aggregation- and season-specific larval production fields

The initial spawning conditions in our model are represented by larval density fields $l(x,y)$, where each x,y position represents a grid cell within the model domain. Larval production fields were estimated within each season and at each particle location in the model (i.e. 1 km^2 grid square within our model domain; see below) using the product of fecundity ($f_{season,size}$) and adult density ($c_{size}(x,y)$) summed over all size classes:

$$l(x,y) = f_{season,small} c_{small}(x,y) + f_{season,medium} c_{medium}(x,y) + f_{season,large} c_{large}(x,y) \quad (3)$$

The middle of the GSC over the deepest part of the channel is rarely surveyed due to consistently low densities of scallops over this large area, possibly due to unsuitable rocky habitat (see Fig. 4, D. Hart pers. comm.), so this small segment was not included as a part of the GSC aggregation, and no larvae were released there.

Particle-tracking model description

Scallop larval transport, behaviour, growth and mortality were simulated on Georges Bank using an enhanced version of the 3D particle-tracking model described in Gilbert et al. (2010). Briefly, in Gilbert et al. (2010), 64 particles were seeded at every 16 km^2 grid node twice yr^{-1} during the mid-point of each spawning period (16 May and 20 September) and within the 3 spawning aggregations defined above

on Georges Bank (Fig. 1). Particles were seeded into a physical environment characterised using monthly climatological currents, turbulence, density and temperature fields derived from the Finite-Volume Coastal Ocean Model (FVCOM; Chen et al. 2003, see next section for description of fields). Particles were assumed to settle at the end of their pelagic larval duration (PLD), and 2 contrasting PLD cases were compared: a constant PLD of 35 d, and a temperature-dependent PLD where local temperature affected growth with a $Q_{10} = 2$. Horizontal transport was governed by horizontal advection, while vertical transport of larvae was simulated using 2 contrasting behavioural assumptions: passive and pycnocline-seeking, consistent with field observations (Tremblay et al. 1994). To implement these cases, Gilbert et al. (2010) first estimated pycnocline depth from the modelled density (ρ) field using a threshold definition of $\Delta\rho = 0.6$ kg m^{-3}, as this value provided estimates of pycnocline depth that were consistent with observations made in September on the NEP (Tremblay & Sinclair 1990, Tremblay et al. 1994). Locations where this threshold was not reached within the upper 40 m of the water column were considered well-mixed, and the particles were placed randomly in the water column in well-mixed regions regardless of the behavioural assumption. In the pycnocline-seeking case, particles in stratified regions remained at the pycnocline, and pycnocline depth was calculated from the water mass density profile interpolated to each particle location and each time step. In the passive case, vertical displacement in stratified regions was simulated by the combination of vertical advection and diffusion, where the latter was calculated from a random walk based on local values of the modelled turbulent mixing coefficient and calculated using the standard Visser algorithm with a time step of 0.75 s (Visser 1997). Particles were initialised at the pycnocline in both behavioural simulations.

The physical environment (i.e. Lagrangian displacements ($dx(x,y,z,t)$,$dy(x,y,z,t)$,$dz(x,y,z,t)$), turbulence, density, temperature) was characterised using output from the FVCOM. FVCOM is an unstructured-grid, primitive-equation, hydrostatic, numerical model that has been shown to perform well in coastal applications (Chen et al. 2003). The model was initialised with monthly mean hydrographic and wind fields using all available data for the Gulf of Maine and Scotian Shelf from the Bedford Institute of Oceanography and National Ocean Data Center databases (Pringle 2006). Tidal currents were driven by the M2 tide, the dominant tidal constituent in the Gulf of Maine/Georges Bank region. Larval paths were calculated from tidal residual displacements obtained by tracking Lagrangian particles over the entire domain in the model after the model had been spun up to a quasi-steady-state circulation for a given forcing, as described by Hannah et al. (1997). In order to reduce computational costs by use of a large advective time step (Δt = M2 semi-diurnal tidal period = 12.42 h), our particle-tracking model input Lagrangian residual quantities (i.e. the average quantity seen by a particle as it is displaced over one tidal cycle; Zimmerman 1979, Johnson et al. 2006, Gilbert et al. 2010). This means that we tracked particles in the online FVCOM model at a 2 min time step, and we did not extract the average velocities over a month from that model, we extracted the average displacements of particles over a tidal time-step from that model. This averaging reduces the influence of the weak temporal variability in the velocity fields on timescales other than the tidal timescales. Model output was interpolated onto a grid with 1 km horizontal resolution (x,y) and 32 (scalar quantities) or 15 (vector quantities) σ-layers (z) in the vertical. Temporal evolution of these fields was simulated by linear interpolation in time between months. These physical fields are an improved version of the fields applied in the tracking model of Johnson et al. (2006): we improved upon them by adding variable winds, and our fields are the same as those used in Gilbert et al. (2010). Both the spring and fall model residual circulation in our physical fields demonstrate the classic Georges Bank features: (1) an anti-cyclonic gyre associated with the tidal mixing front roughly along the 60 m isobaths, which has peak intensity in late summer and early autumn (e.g. Butman & Beardsley 1987), and (2) fast along-shelf currents on the outer flanks roughly between the 60 and 200 m isobaths (Naimie et al. 1994, 2001). Features of the gyre that were captured include the strongest flow in a jet along the Northern Flank, currents generally decreasing with depth below the surface, and north or northwestward flow in the GSC contributing to partial recirculation (Tremblay et al. 1994).

Modifications to horizontal transport

In this study, 2 major enhancements were made to the Gilbert et al. (2010) model to improve the realism of the transport. First, sampling of horizontal variability in the environmental conditions was improved. This was accomplished in 2 ways: (1) by increasing model resolution from 16 to 1 km^2 to match the maximum resolution of the physical

oceanographic model fields (because important smaller-scale processes are grid-size dependent and best captured with the highest possible resolution), and (2) by adding a horizontal random walk to simulate horizontal particle diffusion. The random walk was simulated for each particle over each 12.42 h time step, such that the change in particle position (x_{ind}, y_{ind}) over a time step (Δt) was computed as in Xue et al. (2008):

$$x_{ind}(t + \Delta t) = x_{ind}(t) + dx(x_{ind}, y_{ind}, z_{ind}, t) + \sqrt{(2\ H_z\ \Delta t)} \times R \quad (4)$$

$$y_{ind}(t + \Delta t) = y_{ind}(t) + dy(x_{ind}, y_{ind}, z_{ind}, t) + \sqrt{(2\ H_z\ \Delta t)} \times R \quad (5)$$

where R represents a random number drawn from a standard normal distribution, and H_z represents a constant horizontal diffusivity with a value of 5 m^2 s^{-1}, which is more conservative than diffusivity values calculated in Xue et al. (2008). The literature values are appropriate for small time steps of the random walk (e.g. minutes), but over a tidal time step would result in over-dispersion, because in reality the particles would randomly change direction due to diffusion many times over the tidal cycle. A value of 20 m^2 s^{-1} would thus overestimate the total distance travelled by a particle due to diffusion in some places over a 12.5 h time step. We performed sensitivity analysis on a range of horizontal diffusivities from none to typical literature values (see Section S3 and Fig. S14 in the Supplement). Four particles were released at each 1 km^2 grid node to maintain the same level of individual variation for stochastic vertical motions as in Gilbert et al. (2010), while simultaneously increasing the individual variability in horizontal. For simulations involving larvae rather than particles, local larval density, $l(x,y)$, was divided equally among each of the 4 particles released at a grid node to create the weighted particle distributions.

Modifications to vertical transport

The second modification consisted of 2 components related to vertical transport: empirical characterisation of the pycnocline, and improved realism of the pycnocline-seeking behaviour sub-model. The first component was deemed important after comparison with an empirical dataset revealed that pycnocline depths calculated from the modelled density fields in Gilbert et al. (2010) were too deep, to the extent that during May, October and November the pycnocline in Gilbert et al. (2010) was non-existent in the entire region, while the data demonstrated that a pycnocline was present (see Section S2.1 in the Supplement). This was problematic because characterization of the pycnocline is used to determine the model's initial conditions as well as to delineate between stratified and well-mixed areas for behavioural assumptions and corresponding vertical transports. Here, the pycnocline depth and the boundary separating the stratified and well-mixed zones was not calculated from the modelled density fields, but instead was calculated empirically from data compiled from 7395 CTD profiles collected between 1978 and 2009 within our model domain (Figs. 2 & 3; see Section S1 in the Supplement for methodological details and explanations of spatial and inter-annual variability in this dataset).

Our model was further enhanced by making pycnocline-seeking behaviour stochastic, in contrast to Gilbert et al. (2010) where this behaviour was deterministic with particles always positioned exactly at their local pycnocline depth at every time step. This is an improvement because field observations of larval vertical distribution show that larvae are normally or log-normally distributed in a ~30 to 60 m thick layer around the local pycnocline (Tremblay & Sinclair 1990). To simulate the observed variability in vertical position around the pycnocline, each particle's vertical position in a stratified zone at each 12.42 h time step was randomly selected from a log-normal distribution of seasonal mean pycnocline depth estimated from empirical data (Fig. 3). Pycnocline depth varied by a range of ~40 to 60 m in every month, and larvae can swim vertically between 5 and 60 m over a tidal cycle (0.1 to 1.3 mm s^{-1}; Gilbert et al. 2010); hence using the distribution of pycnocline depths to simulate variation in larval vertical distribution at each time step is appropriate.

To implement this enhancement, the boundary separating the well-mixed and stratified regions was defined using the data from each month during May through November (Fig. 2). The boundary is comprised of ~12 adjoining line segments that approximately encompass several Fisheries and Oceans Canada-generated Gulf of Maine system sub-regions (Fig. S6 in the Supplement; www.bio.gc.ca/science/data-donnees/base/polygons-polygones/scoshelf-scoetageres-eng.php). Particles behaved passively (i.e. vertical advection + turbulence) in the entire domain in the passive simulation, but behaved passively only inside the well-mixed zone during the pycnocline-seeking simulation. Within the stratified zone, each month the mean and variance parameters defining the log-normal probability density function

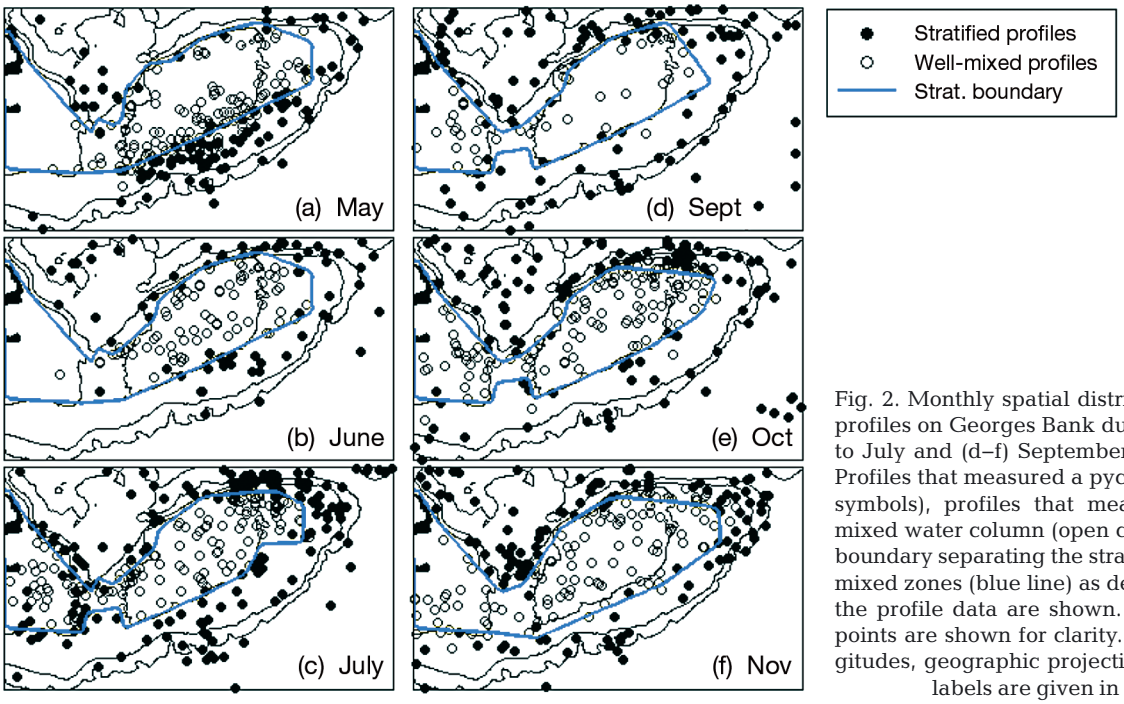

Fig. 2. Monthly spatial distribution of CTD profiles on Georges Bank during (a–c) May to July and (d–f) September to November. Profiles that measured a pycnocline (closed symbols), profiles that measured a well-mixed water column (open circles), and the boundary separating the stratified and well-mixed zones (blue line) as determined from the profile data are shown. One in 5 data points are shown for clarity. Latitudes, longitudes, geographic projection and isobath labels are given in Fig. 1

(PDF) of pycnocline depth from all profiles were calculated (Fig. 3). The boundary and PDF parameters were assumed to represent the environmental conditions at mid-month, and at each time step these were linearly interpolated between the 2 surrounding months in the same manner as the modelled environmental variables (Gilbert et al. 2010). The boundary was interpolated in time and space by linearly interpolating between the vertices at adjoining line segments each month.

Modifications were also made to the implementation of the Visser algorithm for random walk. Errors were corrected in the calculation of the random displacement, which overestimated displacement when particles were located in large diffusivity gradients and underestimated displacement where diffusivity gradients were small. When these issues were corrected, we noted that the algorithm caused accumulation of particles in regions near the top and bottom boundaries where the model diffusivity had sharp gradients, which is a known problem in the Visser algorithm (Brickman & Smith 2002), and the diffusivity fields were subsequently smoothed at the boundaries. Sensitivity analyses confirmed that these modifications had no effect on the conclusions drawn in Gilbert et al. (2010) because vertical diffusion has a negligible effect on aggregation-scale dispersal on the Bank. The results were primarily driven by advection and pycnocline definition, and since we made substantial changes to both of these modelled processes in this study, we provide a detailed model comparison between our improved model and the Gilbert et al. (2010) model in Section S2 in the Supplement.

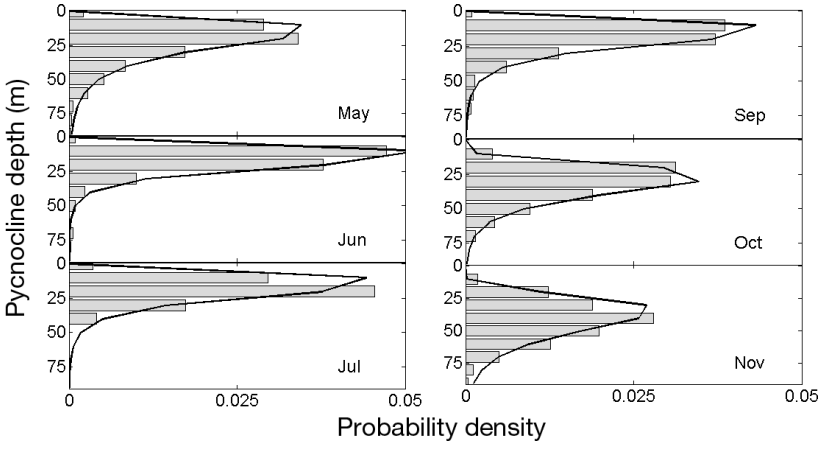

Fig. 3. Monthly (May to June and Sept to Nov) histograms (bars) and log-normal probability density functions (solid line) of pycnocline depth calculated from all profiles within the stratified zone of our model domain in the Georges Bank region (Fig. 1)

Characterizing number of larvae in the model

Each particle in the model was made into a particle-associated cohort of larvae (also commonly called a 'super-individual' as in North et al. 2009) at the beginning of a simulation by weighting each particle by the larval density $l(x,y)$, defined above. Once spawned, the number of larvae (N) associated with a particle decreased over each time step based on the survivorship:

$$N(t+\Delta t) = N(t)e^{-m\Delta t} \quad (6)$$

Initially, larvae were killed off with a constant larval mortality rate (m) of 20% d^{-1}, which lies between the estimates of 15 and 25% for Georges Bank scallop larvae made by Tremblay et al. (1994) and McGarvey et al. (1992), and used in previous modeling studies (e.g. Tian et al. 2009a,b). Subsequent simulations using spatially and temporally varying mortality are described in the Results. Each particle-associated cohort was assumed to have temperature-dependent development and pycnocline-seeking behaviour, which varied among cohorts associated with other particles (i.e. cohorts with other spawning locations and/or different environmental histories).

Characterization of connectivity

At the end of each simulation, particle or larval exchange was summarized by defining a 'dispersal matrix', where each element $e(i,j)$ equals the total number of particles or larvae spawned in aggregation j (where j is GSC, NEP or SF) that settled in region i, where i can be one of the 3 aggregations as well as 'unsuitable habitat' (UH) or, in the case of particles only, 'downstream' (DS). UH was defined as any region outside of adult scallop aggregations but within the model domain, which corresponds to locations where no significant scallop densities are observed (Hart & Chute 2004, Smith et al. 2009) and where the suitability of benthic substrate is low (Tian et al. 2009a). The DS region was defined as all locations outside of the study domain. DS larvae are primarily transported west of 71° W, and represent potential supply to scallop populations southwest of Georges Bank. The DS category is not included in our assessment of larval connectivity because larval growth and mortality cannot be tracked once larvae leave the domain, and meaningful DS connectivity estimates are not possible. For each simulation, we also present the contribution to total annual settlement, where each element $c(i,j)$ equals the fraction of particles or larvae spawned in aggregation j and settling in region i divided by all 6 possible sources to a settlement region (3 aggregations and 2 seasons).

RESULTS

Seasonal, spatial and size-specific variation in larval production

Seasonal variation in larval production on Georges Bank was determined by fecundity rates, whereas spatial variation was influenced by the distribution and size of adult spawning females. Seasonal fecundity rates were approximately twice as high in autumn as in spring, and relative changes in fecundity with size class were not linear; rather, the large scallops were disproportionately more fecund (Table 1). Variation in adult densities occurred both among and within aggregations. Among aggregations, densities were higher on the NEP than either the SF or GSC. Adults in each aggregation were distributed between the 60 and 100 m isobaths in an anisotropic manner, with the major axes of both the scallop aggregations and the highest density patches (10^5 to 10^6 females m^{-2}) within those aggregations directed along-isobath (Figs. 4 & 5). Scallop densities were roughly equal across size classes in the GSC, whereas densities were higher in smaller size classes on the NEP and SF (Fig. 4). Variation in the spatial distribution of adults among size classes occurred within each aggregation. Small and medium-sized scallops were particularly high in concentration (>10^6 females km^{-2}) in the northern region of the NEP, whereas the large scallops were higher in abundance and more homogeneously distributed throughout the southern region of the NEP (Fig. 4). Small and medium-sized scallops were

Table 1. Shell height, age range and season- and size-specific fecundity of sea scallops *Placopecten magellanicus* collected on Georges Bank during spring and autumn. Animals are classified into 3 size classes; the proportion that each size class contributes to the total seasonal fecundity is given and is approximately the same each season

Size class	Shell height (mm)	Approx. age (yr)	Fecundity (no. eggs female^{-1}) Spring	Autumn	Proportion (%)
Small	50–95	2–4	2.09×10^7	3.59×10^7	15–18
Medium	95–120	4–6	3.30×10^7	6.79×10^7	29
Large	120–170	6+	6.13×10^7	13.2×10^7	53–56

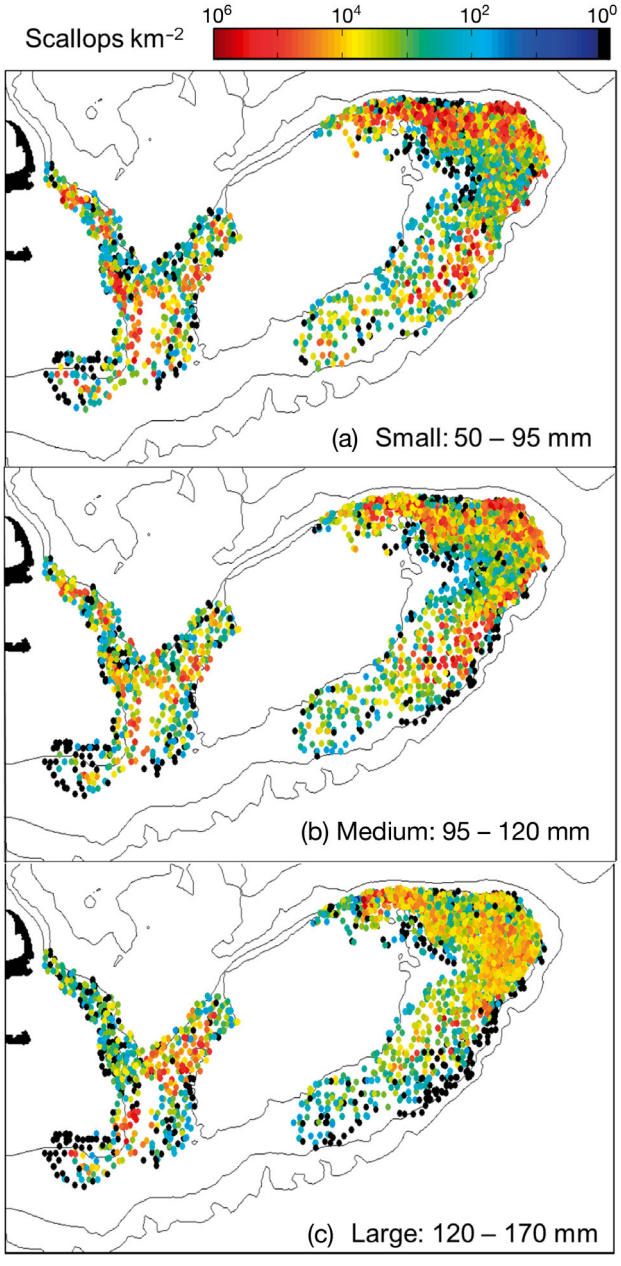

Fig. 4. Scallop abundance km^{-2} collected during 1994 through 2004 on Georges Bank and divided into 3 size classes: (a) small, (b) medium and (c) large. Black symbols indicate tows containing 0 scallops. Latitudes, longitudes, geographic projection and isobath labels are given in Fig. 1

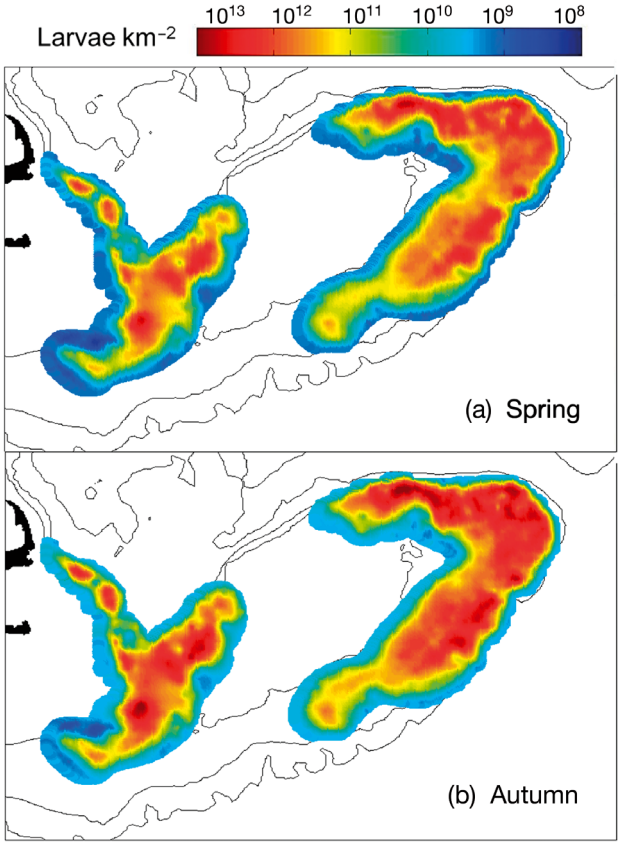

Fig. 5. Spatial distribution of larval production (km^{-2}) kriged at 1 km^2 resolution and integrated over all 3 size classes within each of 3 aggregations (GSC, NEP, SF, see Fig. 1) on Georges Bank during (a) spring and (b) autumn. Latitudes, longitudes, geographic projection and isobath labels are given in Fig. 1

clustered throughout the GSC, whereas the large scallops were primarily aggregated along the northeastern arm. The spatial distribution of all 3 size classes in the SF showed elevated concentrations along the 100 m isobath. Each of the above sources of variation is evident in the resulting larval production (Table 2, Fig. 5). Seasonal larval production was ~10^{15} per aggregation, and was approximately twice as high during autumn compared with spring. The NEP produced the most larvae, roughly the same as the combined amount from the GSC and SF (Table 2). Although the large size classes were the most fecund (Table 1), higher adult densities in the medium size classes (Fig. 4) caused the medium size classes to produce more larvae overall than the large size classes in both the NEP and SF beds in both seasons (Table 2). In the GSC, the largest size class produced the most larvae. To summarize, larval production in spring is on average quite substantial in all aggregations on Georges Bank.

Particle dispersal and connectivity

Variation in scallop larval dispersal between seasons on Georges Bank had a relatively small effect on larval settlement and connectivity compared to intraseasonal spatial variation within and among different

Table 2. Total sea scallop *Placopecten magellanicus* larval production (no. larvae × 10^{15}) on Georges Bank during each spawning period (spring and autumn), size class (see Table 1) and spawning aggregation (GSC, NEP, SF, see Fig. 1)

Season	Size class (mm)	GSC	NEP	SF
Autumn	Small	1.11	2.26	1.17
	Medium	1.20	3.73	1.74
	Large	2.47	3.49	0.92
	Total	4.78	9.48	3.83
Spring	Small	0.64	1.55	0.68
	Medium	0.58	1.81	0.84
	Large	1.15	1.62	0.43
	Total	2.37	4.98	1.95

Table 3. (A) Dispersal matrices summarizing particle and larval settlement within and among 3 aggregations on Georges Bank during autumn and spring under 2 scenarios that define larval mortality (m): constant (m = 20% d^{-1}) and temperature-dependent, $m(T)$. Each column corresponds to a spawning aggregation, and each row corresponds to a settlement region (GSC = Great South Channel, NEP = Northeast Peak, SF = Southern Flank, UH = uninhabitable and, for particles only, DS = downstream). Larvae numbers are ×10^9. The same quantities are then presented in (B) as the relative percent contribution of each spawning aggregation to total annual production in settlement region (i.e. the denominator is the sum of all 6 spawning sources to a settling region over both seasons)

	Particles			Larvae, m = 20% d^{-1}			Larvae, $m(T)$		
	GSC	NEP	SF	GSC	NEP	SF	GSC	NEP	SF
(A) No. of particles/larvae									
Autumn									
GSC	2519	1372	5623	740	226	2256	866	227	1295
NEP	2362	1372	234	371	15	4	602	15	4
SF	787	9258	469	230	1107	2	509	1556	1
UH	3464	22 288	15 697	811	7232	4114	992	7551	2295
DS	6612	0	1171						
Spring									
GSC	787	1029	4920	12	2	38	100	26	392
NEP	1417	343	703	15	0.9	0.6	284	17	9
SF	630	5486	0	5	80	0	116	1177	0
UH	3621	27 431	13 588	33	350	229	518	3458	1368
DS	9446	0	4217						
(B) Contribution to total annual settlement (%)									
Autumn									
GSC	16	8	35	23	7	69	30	8	45
NEP	37	21	4	91	4	1	65	2	0
SF	5	56	3	16	78	0	15	46	0
UH	4	26	18	6	57	32	6	47	14
DS	31	0	5						
Spring									
GSC	5	6	30	0	0	1	3	1	13
NEP	22	5	11	4	0	0	31	2	1
SF	4	33	0	0	6	0	3	35	0
UH	4	32	16	0	3	2	3	21	8
DS	44	0	20						

regions. Retention within our model domain of particles seeded on the SF and NEP was >80% in both seasons, whereas only 40 to 58% of particles seeded on the GSC were retained on-Bank because particles in the northwestern region shallower than the 80 m isobath advected downstream in the along-isobath current within the first few days after seeding (Table 3A, Figs. 6–8). One hundred percent of NEP-seeded particles settled on Georges Bank in both seasons, whereas on-Bank retention of particles seeded on the SF and GSC was higher during autumn. Retention of SF-seeded particles was 13% higher during autumn (95%) than spring (82%), however this difference had little effect on connectivity among aggregations because the majority of autumn-seeded particles settled in UH areas to the southwest of the SF aggregation (Fig. 6). On-Bank retention of GSC-seeded particles was 18% higher during autumn than during spring, which had the effect of increasing the number of particles settling in both the GSC and NEP during autumn relative to spring (Table 3A). In total, twice as many particles (13 663 particles) were advected out of the model domain and downstream during spring compared to autumn (7783; Table 3A), and this is consistent with the interpretation that reduced gyre circulation during spring, particularly in the region of the GSC, causes more spring-spawned larvae to advect downstream presumably to seed populations on the mid-Atlantic Bight.

The most important supplier of particles to an aggregation of scallops on Georges Bank was the aggregation immediately upstream in all simulations (Table 3A). Local retention of particles was low in the NEP (1 to 4%) and SF (0 to 2%). Long pelagic larval duration during spring resulted in NEP-spawned particles overshooting the SF aggregation (Fig. 7), hence only 16% of NEP-seeded particles settled on the SF during spring, compared to 27% during autumn. The overall supply of particles from NEP to SF is significant due to the large area occupied by the NEP aggregation; thus, even though only 16% of NEP-seeded particles settled on the SF during spring, more particles settled on the SF than the NEP during spring or

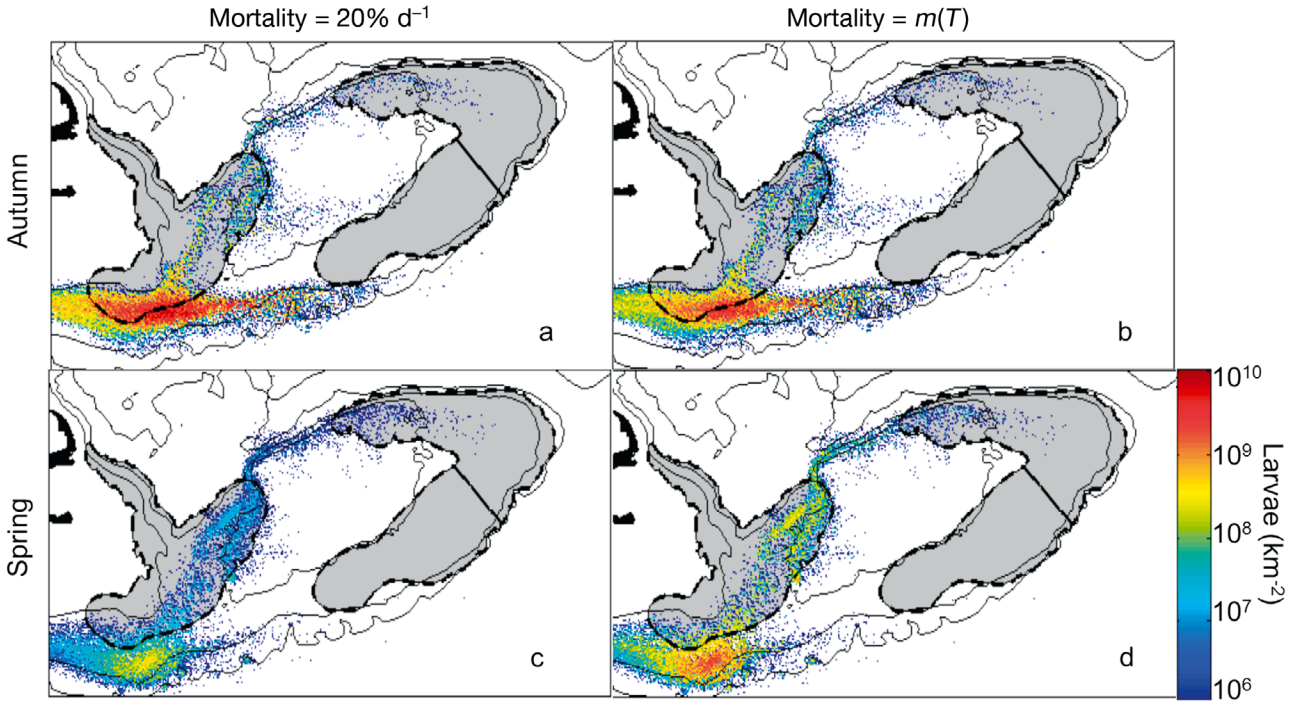

Fig. 6. Settlement distribution of larvae spawned on the Southern Flank of Georges Bank during (a,b) autumn and (c,d) spring, and experiencing (a,c) constant (m = 20% d^{-1}) or (b,d) temperature-dependent ($m(T)$) larval mortality during their pelagic phase. Latitudes, longitudes, geographic projection and isobath labels are given in Fig. 1

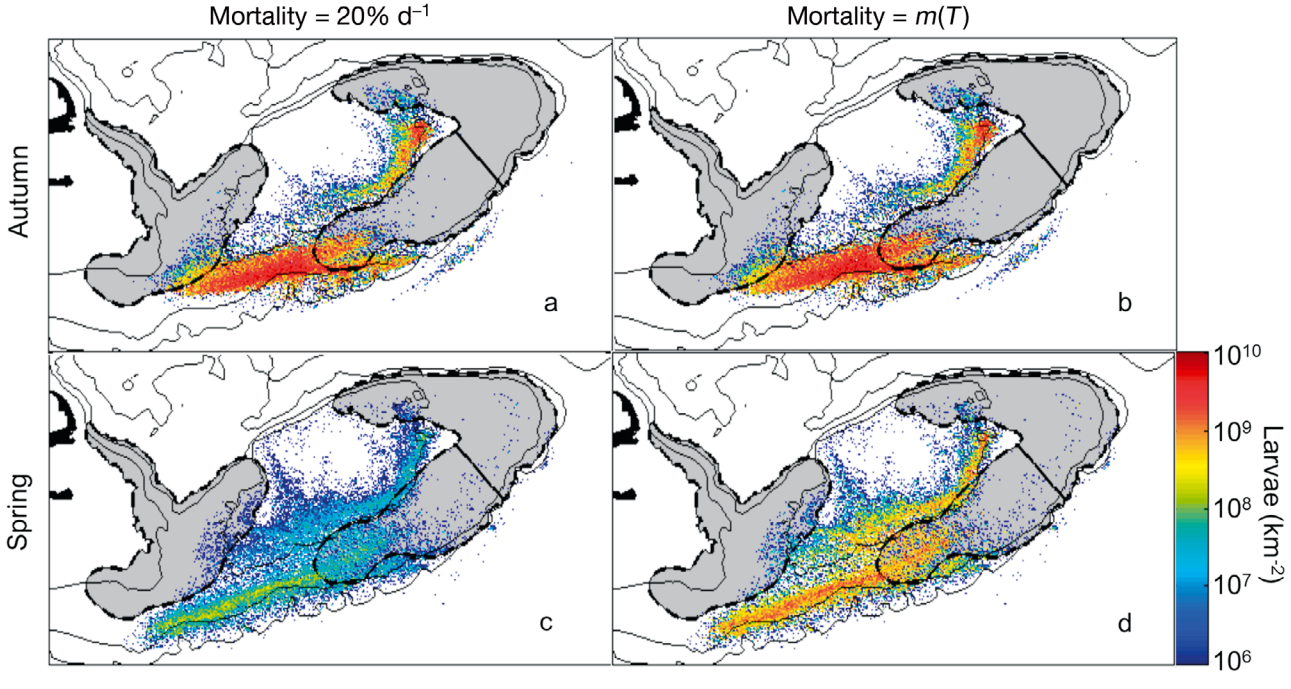

Fig. 7. Settlement distribution of larvae spawned on the Northeast Peak of Georges Bank during (a,b) autumn and (c,d) spring and experiencing (a,c) constant (m = 20% d^{-1}) or (b,d) temperature-dependent ($m(T)$) larval mortality during their pelagic phase. Latitudes, longitudes, geographic projection and isobath labels are given in Fig. 1

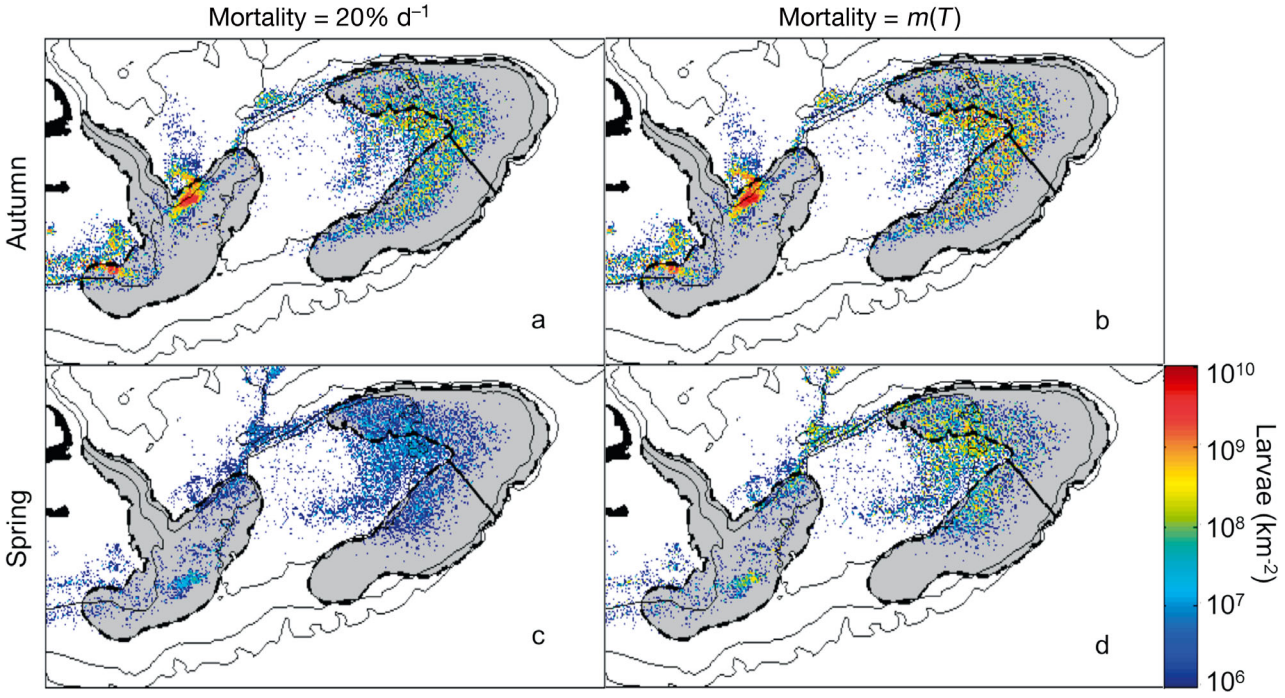

Fig. 8. Settlement distribution of larvae spawned in the Great South Channel of Georges Bank during (a,b) autumn and (c,d) spring and experiencing (a,c) constant (m = 20% d^{-1}) or (b,d) temperature-dependent ($m(T)$) larval mortality during their pelagic phase. In each modelling scenario, pycnocline-seeking behaviour and an individually varying, temperature-dependent pelagic larval duration were assumed. Latitudes, longitudes, geographic projection and isobath labels are given in Fig. 1

autumn (Table 3A). All GSC-seeded particles settled within the 80 m isobath and on the northwestern portion of the NEP, regardless of season (Fig. 8), suggesting that larval supply to the eastern and southern regions is negligible despite the fact that many small adults are found in both regions (Fig. 4). Strong settlement along the northern region of the NEP could help explain why this area has higher numbers of small scallops than in the southern region (Fig. 4).

The greatest supplier of particles to the GSC was the SF (65% of all particles annually; Table 3B). These settled particles were concentrated in the southernmost region of the GSC in a narrow, along-isobath strip between the 70 and 80 m isobaths that ran through the middle of the GSC and then turned east along the northern flank (Fig. 6). This distribution is consistent with the distribution of the adult patches in those areas, which are oriented along isobath and have elevated concentrations in the middle of the bed (Fig. 4). The SF did not supply the northwestern region of the GSC aggregation; rather, this area was supplied by local retention of particles within the GSC (Fig. 8). There seems to be no larval supply from Georges Bank to the northwest arm that extends toward the Cape Cod Bay (Figs. 6–8), although small scallop densities are significant in that region, suggesting alternate supply sources (Fig. 4).

Taken together, these results show a general reduction in connectivity during spring compared to autumn; however, a considerable number of particles settled within each aggregation during spring, and the difference in retention between seasons was smaller than the spatial variation in larval sources both among aggregations and within the GSC aggregation. Downstream losses were higher during spring, which primarily affected the GSC and had a small effect on the NEP and SF aggregations. Thus, based solely on transport processes, it seems that the spring spawn could still make a significant contribution to total annual larval settlement on Georges Bank.

Effect of heterogeneous larval production on settlement distributions

Weighting each particle by locally spawned larval density (hereafter referred to as simulated 'larvae') somewhat changed the conceptual picture of connectivity compared to simulating un-weighted particles (Table 3A). Simulating larvae instead of particles caused local retention to decrease substantially in all aggregations during autumn (GSC–GSC: –13%, NEP–NEP: –16%, SF: –6%). This affected the GSC in particular, where transport processes promoted strong

local retention of particles in the northwestern regions of the aggregation, but fewer large adults resulted in relatively lower production in that area (Table 3A, Figs. 4 & 8). Similar to particles, the strongest connections were the immediate upstream–downstream connections; however, the GSC contributed substantially to all 3 aggregations. Considering larvae rather than particles caused the strength of the GSC–NEP connection to increase by 20 to 22% regardless of the mortality scenario or season (Table 3A). The strength of the NEP–SF connection also increased, particularly during spring, by 11 to 14% depending on the mortality scenario. This occurred because particles tended to advect through and past the SF aggregation in spring; however, larval production on the NEP is concentrated in the northern region, so particles arriving last to the SF were weighted with more larvae and did not have time to advect past the aggregation before settling. The strength of the SF–GSC connection generally stayed the same between particle and larval simulations, but in one instance also increased (autumn, constant mortality). The strength of the GSC–NEP and NEP–SF connections increased in larvae over particles because spawning adults were aggregated along the flanks between the 60 to 100 m isobaths, precisely where the gyre circulation joining the aggregations is strongest (this may also be why local retention decreased during autumn). The SF–GSC connectivity was in 3 of 4 cases similar between larvae and particles, because although scallops are aggregated, the high density patch occurs near the 100 m isobath (Fig. 4) and many larvae from that aggregation are advected into uninhabitable areas and downstream (Fig. 6). Outside of the patch, larval production was relatively homogeneous (i.e. closer to the distribution of particles) throughout the aggregation compared to the other 2 aggregations (Fig. 4).

Effect of variable mortality rate on spring survivorship

Since production in spring is about 50% of autumn production across the entire Bank, if only production were considered, spring larval settlement should be about half of autumn settlement. Thus, based on seasonal variation in production alone, the spring spawn makes a significant contribution (about one-third) on average to total Bank settlement. If an argument is to be made that the spring spawn makes a negligible contribution to total annual recruitment, this argument must be defensible primarily on seasonal variation in larval mortality.

Results from simulations using constant mortality are consistent with the present conceptual paradigm that the contribution of the spring spawn to overall annual larval settlement on Georges Bank is negligible compared to autumn. Spring spawning only contributed 1 to 6% to total annual settlement within any of the 3 settlement aggregations (Table 3B). Notably, only 1% of larval settlement on the GSC occurred in spring. Low spring settlement can be attributed in part to the combination of lower fecundity in spring. The bigger factor is that spring-spawned larvae are subject to mortality for ~12 d longer than in autumn (35 vs. 48 d). For an instantaneous mortality rate of 20% d^{-1}, 12 additional days translates to a decrease in survivorship of >90%, and only 9% of those survived through Day 35 will still survive through Day 48. These results imply that lower fecundity combined with higher cumulative mortality in spring means there may be no recruitment benefit to a spring spawn, which leads to the questions: why does a spring spawn recur almost every year, and why do scallops expend one-third of their reproductive resources on average during the spring spawn?

The mortality of meroplankton such as scallop larvae is typically attributed to biotic factors such as predation and starvation, as well as abiotic factors that lead to physiological stress, such as temperature or salinity (Metaxas & Saunders 2009). A meta-analysis identified a positive correlation between temperature and mortality rates across 23 different taxa (Houde 1989). Houde & Bartsch (2008) suggested that in the absence of species-specific data on the relationship between temperature and mortality, a relationship between the 2 should be assumed. Since no data on larval mortality rates are available for *Placopecten magellanicus*, survivorship was estimated at each time step using Eq. (6), where m in that equation is now based on the local temperature $m(T)$ via an exponential (Q_{10}) relationship:

$$m(T) = m_0 Q_{10}^{(T-T_0)/10} \quad (7)$$

where m_0 is the mortality rate at the reference temperature T_0, chosen here to be the same as the constant rate of 20% d^{-1} for the mean fall temperature (13.5°C). Since there are no data to support a specific choice for the Q_{10} factor, we chose a Q_{10} = 2 to illustrate the outcome if the temperature dependency of larval survivorship is the same as that assumed for growth in each season. This simulates equal survivorship between seasons, because the colder temperatures in spring vs. autumn result in a lower instantaneous mortality rate that is approximately cancelled by the corresponding longer PLD (see

Fig. S15 in the Supplement at www.int-res.com/articles/suppl/m516p209_supp.pdf). This assumption about mortality rate is intended to be illustrative, and does not necessarily reflect the true seasonal difference in mortality rates. The goal is to simply illustrate the effect that plausible spatial and inter-seasonal differences in the mortality have on larval connectivity, without explicitly modeling the mechanisms that cause these changes.

Subjecting larvae to temperature-dependent mortality rather than constant mortality caused total survivorship to change in both seasons, however the effect was small in autumn and large in spring (Table 3A, Figs. 6–8). Larval survivorship in spring increased by 1 to 2 orders of magnitude when subjected to temperature-dependent rather than constant mortality (Table 3A). Under variable mortality, the spring spawn contributed 18, 33 and 38% to the total settlement within the GSC, NEP and SF aggregations, respectively, and contributed 13 to 35% of the total annual production between the immediate upstream–downstream connections (GSC to NEP, NEP to SF, and SF to GSC) (Table 3B). The number of spring recruits increased in every settlement region because cold spring water temperatures (~9.5°C) led to average temperature-dependent mortality rates of ~15.7% d^{-1} (range: 15.0 to 16.8%). Survivorship increased most dramatically in larvae spawned on the NEP and settled in the SF because the coldest water temperatures (5 to 7.5°C), and therefore the lowest mortality rates (~11% d^{-1}) on Georges Bank were on the NEP during spring.

During autumn, the average water temperature experienced by particles was close to the reference temperature of 13.5°C (~12.9°C; Gilbert et al. 2010 their Fig. 2). Consequently, the average temperature-dependent mortality rate experienced by larvae during autumn was similar to the base mortality rate (19.2% d^{-1}, range: 18.3 to 20.5%). Larval survivorship then varied little between mortality scenarios (within an order of magnitude), and regional variability in temperature caused total survivorship at settlement to increase in some regions and decrease in others relative to the constant mortality case. Temperatures in the southeastern region of the SF surpassed 13.5°C during autumn, therefore larvae that transited this area (i.e. SFL → GSC and SFL → UH) experienced temperature-dependent mortality rates of up to 25% d^{-1}. Furthermore, as the spawning beds of these larvae were immediately upstream of this warm region, larvae experienced high mortality rates shortly after birth (near beginning of PLD), so a greater number of larvae died than if high mortality rates had occurred near the end of their PLD (e.g. GSC-spawned larvae). Consequently, overall survivorship on the SF was lower in these cases compared to the constant mortality scenario (Table 3A, Fig. 6a,b). Larvae that did not pass through the southeastern region of the SF (i.e. all GSC-spawned larvae, NEP → SF) encountered temperatures lower than 13.5°C, therefore temperature-dependent mortality rates experienced by larvae were consistently lower than 20% d^{-1} and survivorship increased for these cases (Table 3A, Figs. 7 & 8a,b).

Although the NEP exhibited the highest production on Georges Bank during autumn, it contributed surprisingly few larvae to settlement within the population (i.e. the 3 parent aggregations). Only 16 to 19% of larvae spawned on the NEP settled within the 3 aggregations during autumn (regardless of mortality scenario), compared to the 35 to 60% retention within the population from other aggregations (Table 3A); the rest settled in uninhabitable areas either on-Bank or to the southwest of the SF (Fig. 7). When mortality was constant, the SF contributed twice as many larvae to total settlement within the population (2.3×10^{12}) as each of the other aggregations (1.3×10^{12} each) (Table 3A). When mortality was temperature-dependent, the GSC contributed the most larvae to the population (2×10^{12}), and the SF contributed the least (1.3×10^{12}), because water temperatures are coldest (hence, mortality rates lowest) along the Northern Flank and warmest along the SF. During spring, however, the NEP does make a greater contribution of larvae to the population than other aggregations, regardless of mortality scenario. Compared to autumn, relatively more NEP-spawned larvae were retained within the population while relatively fewer were retained from other aggregations. When mortality was constant, the NEP contributed 8.3×10^{10} larvae, more than the other 2 aggregations combined (GSC: 3.2×10^{10}; SF: 3.9×10^{10}). When mortality was temperature-dependent, the effect marginally increased (NEP: 1.2×10^{12}; GSC: 5.0×10^{11}; SF: 4.0×10^{11}).

DISCUSSION

Production and dispersal during autumn

Our autumn larval simulations yielded similar large-scale larval connectivity patterns among Georges Bank scallop aggregations as in previous studies (Tremblay et al. 1994, Tian et al. 2009a,b, Gilbert et al. 2010). These studies all showed that for larvae exhibiting some kind of pycnocline-seeking behaviour (each

study described this behaviour differently), the largest larval source to an aggregation was the aggregation immediately upstream, although the GSC also contributed a significant amount to local retention. The details of the connectivity values were relatively insensitive to varying assumptions about bottom-searching and ascent/descent behaviours because these occur on very short time scales (Tremblay et al. 1994), but were sensitive to assumptions about growth rates, vertical swimming behaviour, the physical environmental forcing and mortality (Tremblay et al. 1994, Tian et al. 2009a,b, Gilbert et al. 2010).

Both the present study and Tremblay et al. (1994) found larval production to be higher on the NEP than on the SF or in the GSC combined, due to the relatively high adult density on the northern region of the NEP. As a consequence, the contribution of the NEP to both the SF and UH areas doubled relative to other sources when dispersal of particle-associated cohorts of larvae was simulated instead of particles. However, we found that a substantial number of these larvae are lost to uninhabitable areas south of the SF aggregation or on the Bank crest, meaning that this large source of production does not contribute proportionally more to Bank recruitment than other aggregations during autumn. This is in contrast to Tremblay et al. (1994), who found that the NEP nearly always contributed the greatest number of larvae to settlement within the Georges Bank population. We used higher resolution, heterogeneous production fields and spatial aggregation definitions, whereas Tremblay et al. (1994) assessed only inter-aggregation variation in production. For comparison, we simulated inter-aggregation variation in production (i.e. spatially homogenous within an aggregation) as an initial condition to see if this yielded the same results as Tremblay et al. (1994). The general connectivity structure did not change, however, we found that the NEP became a more significant source to the GSC and NEP, contributing 20 and 27%, respectively, where the fully resolved production fields yielded an NEP contribution of 7 and 4%. This occurs because larval production on the NEP is concentrated in the northern region, far away from the GSC along the Bank-gyre advective pathway compared to the southwestern region. Consequently, assuming an equal concentration of larvae between these 2 regions would result in a higher contribution of larvae to the GSC than if the heterogeneous distribution is fully resolved. This may help explain why Tremblay et al. (1994) found that the NEP contributed the most larvae to the population during autumn, while we did not.

Agreement between our study, which uses a simplified, climatological physical model, and Tian et al. (2009a,b) who used a state-of-the-art, high resolution physical model, suggests that our simplified model is sufficient to capture the large-scale connectivity on the Bank, which is driven primarily by the large-scale mean circulation. Tian et al. (2009b) conducted a series of model sensitivity investigations to examine the level of impact that simplification of FVCOM physical forcing produces when applied to scallop larval tracking on Georges Bank during autumn. The authors (Tian et al. 2009b) compared larval dispersal and settlement in the state-of-the art model with fully spatially resolved, high frequency forcings and multiple tidal constituents (their Expt 1), with models forced only from M2 tide (as in our climatological modeled fields, Expt 2), or forced with constant density (similar to the seminal Tremblay et al. 1994 larval tracking model, Expt 3). For a particle released in the surface layer anywhere on the Bank, Expt 1 predicted that the particle was retained on the Bank, whereas Expts 2 and 3 showed that it moved southward along the 60 m isobath and out of the study domain in the region of the GSC. This shows that a surface-layer recirculation mechanism in the GSC region is not captured by the simplified models. Agreement among models is better in the bottom layer; however, in the eastern GSC a particle in Expt 1 advects eastward around the northern flank while particles in Exps 2 and 3 advect westward out of the domain, and particle settlement on the crest is higher in Expts 2 and 3. Overall, settled particle distributions were found to be similar among model configurations on the Bank flanks, but it is likely that GSC–NEP connectivity will be underestimated with our simplified physical fields, and settlement on the crest (which is uninhabitable habitat) will be overestimated when compared to the comprehensive model. We used these climatological fields here to focus on elucidating the first-order biological processes influencing larval dispersal and settlement, and we have shown that variation in production and mortality can affect connectivity by up to 22%, and that variation in mortality assumptions can affect larval survivorship by a factor of 20, where the latter had a far larger effect on settlement than variation in the physics. This calls for more empirical studies that quantify environmental variation on larval mortality.

Spawning seasonality and larval mortality

In this paper, we asked why approximately 30% of annual reproductive output is attributable to

spring spawning (DiBacco et al. 1995) if spring-spawned larvae have little value in terms of reproductive fitness. Our simple model shows that if mortality rates are correlated with environmental factors that result in lower survivorship during autumn than in spring, then larval settlement during spring can contribute substantially to total annual larval settlement. Is there reason to suspect that mortality rates may be higher during autumn than during spring? We have shown that if larval mortality rates correlate positively with temperature, as has been demonstrated in other studies (Houde 1989, Morse 1989, Pepin 1991), then temperature-dependent mortality will be higher during autumn. Both predation and food vary depending upon the ecosystem structure and composition as well as the physical landscape, all of which are spatially variable and exhibit annual cycles that cause variation between spring and autumn on Georges Bank. The strength, duration and species composition of phytoplankton (larval food) has a predictable seasonal cycle that has markedly different dynamics between spring and autumn. The seasonal cycle is dominated by spring diatom bloom peaking in April, followed by dinoflagellate dominance elevated throughout the summer between May and September with a pulse during late-autumn (Kane 2011, O'Reilly & Zetlin 1998). The diversity of copepod zooplankton in the Gulf of Maine generally increases from spring to autumn, punctuated at times with local minima during blooms of dominant species such as *Calanus finmarchicus*, *Temora longicornis*, and *Centropages typicus* (Johnson et al. 2011). While much less is known about the seasonal distributions of potential larval predators on Georges Bank (e.g. euphausiids, larval and juvenile fish, jellies) they too exhibit differences in their ecologies between spring and autumn that would affect their predation pressure on scallop larvae. Seasonal variation occurs in the presence of larval fish that rely on the early developmental stages of *Calanus* as a primary food source, and also feeding cycles of planktivorous fish such as herring and mackerel that prey primarily on older copepodid stages (Johnson et al. 2011). Atlantic cod *Gadus morhua* and haddock *Melanogrammus aeglefinus* spawn on Georges Bank in late-winter through spring (Mountain et al. 2008), whereas Atlantic herring *Clupea harengus* are primarily autumn spawners (Jech & Stroman 2012), and the young of any of these species could exert predation pressure on the relatively smaller scallop larvae. The planktivorous euphausiid *Meganyctiphanes norvegica* is noted for forming large surface swarms during warm months of the year in the Gulf of Maine (Johnson et al. 2011). There is much anecdotal but very little quantitative information about the landscape of factors affecting larval mortality on Georges Bank, and directed research in this area will help quantify mortality rates between seasons.

Future directions: a framework for investigating semi-annual spawning adaptation

Our model suggests that a more thorough characterization of the landscape of factors affecting mortality would be helpful in determining how variation in larval production and recruitment are linked during bi-seasonal spawning events. Ecological and evolutionary theoretical frameworks that seek to explain the adaptive significance of this relatively uncommon (in the marine realm) life history strategy can be used to develop testable hypotheses that guide future work. Risk aversion, or 'bet-hedging' is a well-studied theoretical framework proposed to explain the development of such a life history in a diversity of organisms from flowers to insects (Slakin 1974, Philippi & Seger 1989). Bet-hedging is the idea that unpredictably variable environments favour genotypes with lower variance in fitness at the cost of lower arithmetic mean fitness (Simons & Johnstone 2003). Variance in fitness can be reduced by life history strategies that spread the risk of encountering an unfavourable environment over time (Hopper 1999). An individual could spawn the maximum amount of offspring in a single annual event (the 'risk-taker'), and if conditions are favourable a large proportion of those offspring survive, but at the risk of them all dying if conditions are unfavourable. Individuals that bet-hedge have more than one spawning event in a year at the expense of a smaller number of offspring being produced (energy and time cost). This lowers overall annual offspring production, but, over a large number of spawning events, also decreases variance in the number of surviving offspring.

Scallops on Georges Bank are exposed to strong variation in their biological and physical environment among seasons and among years that can drive the evolution of risk-aversion strategies. Since the autumn spawn is generally the more consistent spawn on Georges Bank, one might expect this to be the bet-hedge spawn and uncorrelated to environmental variation, while the magnitude of the spring spawn, which varies strongly among years, may be more closely related to the environmental variation. This

hypothesis can be addressed, and others generated, by looking at the environmental and physiological cues that spawners use to determine how to allocate resources among seasons, and at the environmental factors that drive recruitment variation after spawning, which prominently includes characterising larval mortality effects. Concerning the former, the scallop gametic growth phase may occupy several months of the reproductive cycle (DiBacco et al. 1995), and the timing of this process must be such as to generate a population of mature gametocytes at the appropriate time — either the time when environmental spawning signals will be received, or more importantly, the time when spawning success would be highest (Olive 1995). Seasonal allocation of reproductive resources may then be a function of both the environment and the physiological state of the reproductive individual with respect to gamete production. Concerning the latter, risk aversion suggests that the adult scallop can interpret to some extent environmental cues (or proxies thereof) of larval mortality risk, and modify their reproductive output accordingly. The seasonal landscape of larval food and predation on Georges Bank needs to be characterised to estimate larval mortality in space and time to assess how spawning signals and larval survivorship are linked.

CONCLUSIONS

This is the first modeling study of scallop larvae on Georges Bank that has explicitly considered the interactions between spatial and seasonal variation in larval production and mortality in relation to larval transport processes. We have demonstrated that variation in larval production changes our conception of connectivity among aggregations relative to particle tracking. Processes that affect larval production (e.g. size-selective fishing) can change connectivity, and this should be quantified in future studies. Our simple mortality experiment shows that larval survivorship and settlement distributions are highly sensitive to mortality assumptions, which can drastically change our conceptual understanding of larval recruitment on the Bank. There is no *a priori* reason to believe that mortality is constant between seasons or in space, and conclusions about the importance of the spring spawn that have been drawn from previous studies using constant mortality have not recognized the influence of this extremely important process. More empirical work is needed on mortality to quantify mortality rates for use in these models.

Acknowledgements. Thank you to the scallop stock assessment division at the Bedford Institute of Oceanography, Stephen Smith and Deborah Hart for providing scallop tow data. Thank you to Brittney Vujcich for assisting in model development. We are grateful to Jamie Pringle and Changsheng Chen for providing the physical model, to Chad Gilbert for developing an earlier iteration of the scallop biological model and to 3 anonymous reviewers for providing comments. Funding provided by NSERC Discovery Grant to W.C.G. and by Fisheries and Oceans Canada's Ecosystem Research Initiative to C.D.B. and C.L.J.

LITERATURE CITED

Beaumont AR (1982) Geographic variation in allele frequencies at three loci in *Chlamys opercularis* from Norway to the Brittany coast. J Mar Biol Assoc UK 62:243–261

Brand AR (2006) Scallop ecology: distributions and behaviour. In: Shumway SE, Parsons GJ (eds) Scallops: biology, ecology and aquaculture. Elsevier, Amsterdam, p 651–744

Brickman D, Smith PC (2002) Lagrangian stochastic modeling in coastal oceanography. J Atmos Ocean Technol 19: 83–99

Brown CA, Holt SA, Jackson GA, Brooks DA, Holt GJ (2004) Simulating larval supply to estuarine nursery areas: How important are physical processes to the supply of larvae to the Aransas Pass Inlet? Fish Oceanogr 13:181–196

Butman B, Beardsley R (1987) The physical oceanography of Georges Bank: introduction and summary. In: Backus RH (ed) Georges Bank. MIT Press, Cambridge, MA, p 88–98

Chen C, Liu H, Beardsley R (2003) An unstructured grid, finite-volume, three-dimensional, primitive equations ocean model: application to coastal ocean and estuaries. J Atmos Ocean Technol 20:159–186

Cowen RK, Lwiza KMM, Sponaugle S, Paris CB, Olson DB (2000) Connectivity of marine populations: open or closed? Science 287:857–859

DiBacco C, Robert G, Grant J (1995) Reproductive cycle of the sea scallop, *Placopecten magellanicus* (Gemlin 1971) on northeastern Georges Bank. J Shellfish Res 14:56–69

DuPaul WD, Kirkley JE, Schmitzer AC (1989) Evidence of a semiannual reproductive cycle for the sea scallop, *Placopecten magellanicus* (Gemlin 1971), in the mid-Atlantic region. J Shellfish Res 8:173–178

Edwards KP, Hare JA, Werner FE, Seim H (2007) Using 2-dimensional dispersal kernels to identify the dominant influences on larval dispersal on continental shelves. Mar Ecol Prog Ser 352:77–87

Gaylord B, Gaines SD (2000) Temperature or transport? Range limits in marine species mediated solely by flow. Am Nat 155:769–789

Gilbert CS, Gentleman WC, Johnson CL, DiBacco C, Pringle JM, Chen C (2010) Modelling dispersal of sea scallop (*Placopecten magellanicus*) larvae on Georges Bank: the influence of depth distribution, planktonic duration and spawning seasonality. Prog Oceanogr 87:37–48

Hannah CG, Naimie CE, Loder JW, Werner FE (1997) Upper-ocean transport mechanisms from the Gulf of Maine to Georges Bank, with implications for *Calanus* supply. Cont Shelf Res 17:1887–1911

Hare JA, Churchill JH, Cowen RK, Berger TJ and others (1999) Routes and rates of larval fish transport from the southeast to the northeast United States continental shelf. Limnol Oceanogr 47:774–1789

Hart DR, Chute AS (2004) Essential fish habitat source document: sea scallop, *Placopecten magellanicus*, life history and habitat characteristics, 2nd edn. NOAA Tech Memo NMFS NE-189. Northeast Fisheries Science Center, Woods Hole, MA

Hopper KR (1999) Risk-spreading and bet-hedging in insect population biology. Annu Rev Entomol 44:535–560

Houde E (1989) Comparative growth, mortality and energetics of marine fish larvae. Fish Bull 87:471–495

Houde E, Bartsch J (2008) Mortality. In: North EW, Gallego A, Petitgas P (eds) Manual of recommended practices for modelling physical-biological interactions during fish early life. ICES Cooperative Research Report, Denmark, p 45–63

Jech JM, Stroman F (2012) Aggregative patterns of prespawning Atlantic herring on Georges Bank from 1999-2010. Aquat Living Resour 25:1–14

Johnson CL, Pringle J, Chen C (2006) Transport and retention of dormant copepods in the Gulf of Maine. Deep-Sea Res II 53:2520–2536

Johnson CL, Runge JA, Curtis KA, Durbin EG and others (2011) Biodiversity and ecosystem function in the Gulf of Maine: pattern and role of zooplankton and pelagic nekton. PLoS ONE 6:e16491

Kane J (2011) Multiyear variability of phytoplankton abundance in the Gulf of Maine. ICES J Mar Sci 68:1833–1841

Langton R, Robinson W, Schick D (1987) Fecundity and reproductive effort of sea scallops *Placopecten magellanicus* from the Gulf of Maine. Mar Ecol Prog Ser 37:19–25

MacLeod JAA, Thorpe JP, Duggan NA (1985) A biochemical genetic study of population structure in the queen scallop (*Chlamys opercularis*) stocks in the northern Irish Sea. Mar Biol 87:77–82

Mason J (1983) Scallop and queen fisheries in the British Isles. Fishing New Books, Farnham

McGarvey R, Serchuk FM, McLaren I (1992) Statistics of reproduction and early life history survival of the Georges Bank sea scallop (*Placopecten magellanicus*) population. J Northwest Atl Fish Soc 13:83–99

Metaxas A, Saunders M (2009) Quantifying the "bio-" components in biophysical models of larval transport in marine benthic invertebrates: advances and pitfalls. Biol Bull 216:257–272

Morse WW (1989) Catchability, growth and mortality of larval fishes. Fish Bull 87:417–446

Mountain D, Green J, Sibunka J, Johnson D (2008) Growth and mortality of Atlantic cod *Gadus morhua* and haddock *Melanogrammus aeglefinus* eggs and larvae on Georges Bank, 1995 to 1999. Mar Ecol Prog Ser 353:225–242

Naidu KS, Anderson JT (1984) Aspects of scallop recruitment on St. Pierre Bank in relation to oceanography and implications for resource management. Can Atl Fish Sci Advis Comm Res Doc 84/29. Fisheries and Oceans Canada, St. John's

Naimie CE, Loder JW, Lynch DR (1994) Seasonal variation of the three-dimensional residual circulation on Georges Bank. J Geophys Res 99:15967–15989

Naimie C, Limeburner R, Hannah C, Beardsley R (2001) On the geographic and seasonal patterns of the near-surface circulation on Georges Bank — from real and simulated drifters. Deep-Sea Res II 48:501–518

North EW, Gallego A, Petitgas P (eds) (2009) Manual of recommended practices for modelling physical-biological interactions during fish early life. ICES Cooperative Research Report, Denmark

O'Reilly JE, Zetlin C (1998) Seasonal, horizontal, and vertical distribution of phytoplankton chlorophyll *a* in the northeast US continental shelf ecosystem. NOAA Tech Rep NMFS 139, US Dep Commer, Seattle, WA

Olive PJW (1995) Annual breeding cycles in marine invertebrates and environmental temperature: probing the proximate and ultimate causes of reproductive synchrony. J Therm Biol 20:79–90

Paris CB, Cowen RK, Claro R, Lindeman KC (2005) Larval transport pathways from Cuban snapper (Lutjanidae) spawning aggregations based on biophysical modeling. Mar Ecol Prog Ser 296:93–106

Paris CB, Chérubin LM, Cowen RK (2007) Surfing, spinning, or diving from reef to reef: effects on population connectivity. Mar Ecol Prog Ser 347:285–300

Paulet YM, Lucas A, Gerard A (1988) Reproductive and larval development in two *Pectin maximus* (L.) populations from Brittney. J Exp Mar Biol Ecol 119:145–156

Pepin P (1991) Effect of temperature and size on development, mortality, and survival rates of the pelagic early life history stages of marine fish. Can J Fish Aquat Sci 48: 503–518

Philippi T, Seger J (1989) Hedging one's evolutionary bets, revisited. Trends Ecol Evol 4:41–44

Pineda J, Hare JA, Sponaugle SU (2007) Larval transport and dispersal in the coastal ocean and consequences for population connectivity. Oceanography 20:22–39

Pringle JM (2006) Origins of inter-annual variability in the circulation of the Gulf of Maine. Deep-Sea Res II 53: 2457–2476

Ribeiro P Jr, Diggle P (2001) geoR: a package for geostatistical analysis. R News 1:15–18

Roughgarden J, Gaines S, Possingham H (1988) Recruitment dynamics in complex life cycles. Science 241:1460–1466

Sastry AN (1970) Reproductive physiology variation in latitudinally separated populations of the bay scallop *Aequipecten irradians* Lamarck. Biol Bull 138:56–65

Sastry AN 1979 Pelecypoda (excluding Ostreidae). In: Giese AD, Pearse JS (eds) Reproduction in marine invertebrates. Academic Press, New York, NY, p 113–292

Schmitzer AC, DuPaul WD, Kirkley JE (1991) Gametogenic cycle of sea scallops, *Placopecten magellanicus* (Gemlin 1971), in the Mid-Atlantic Bight. J Shellfish Res 10:221–228

Simons AM, Johnstone MO (2003) Suboptimal timing of reproduction in *Lobelia inflata* may be a conservative bet-hedging strategy. J Evol Biol 16:233–243

Sinclair M, Mohn RK, Robert G, Roddick DL (1985) Considerations for the effective management of Atlantic scallops. Can Tech Rep Fish Aquat Sci 1382:1–113

Slakin M (1974) Hedging one's evolutionary bets. Nature 250:704–705

Smith SJ, Denton C, Hubley B, Jonsen ID and others (2009) Scallop fishing area 29: stock status and update for 2009. Can Sci Advis Sec Res Doc 2009/38, Fisheries and Oceans Canada, Dartmouth

Taylor AC, Venn TJ (1979) Seasonal variation in weight and biochemical composition of the tissues of the queen scallop from the Clyde Sea area. J Mar Biol Assoc UK 59: 605–621

Tian RC, Chen C, Stokesbury KDE, Rothschild BJ and others (2009a) Modeling the connectivity between sea scallop populations in the Middle Atlantic Bight and over Georges Bank. Mar Ecol Prog Ser 380:147–160

Tian RC, Chen C, Stokesbury KDE, Rothschild BJ and others (2009b) Sensitivity analysis of sea scallop (*Placopecten*

magellanicus) larvae trajectories to hydrodynamic model configuration on Georges Bank and adjacent coastal regions. Fish Oceanogr 18:173–184

Tremblay MJ, Sinclair M (1990) Sea scallop *Placopecten magellanicus* larvae on Georges Bank: vertical distribution in relation to water column stratification and food. Mar Ecol Prog Ser 61:1–15

Tremblay MJ, Sinclair M (1992) Planktonic sea scallop larvae (*Placopecten magellanicus*) in the Georges Bank region: broadscale distribution in relation to physical oceanography. Can J Fish Aquat Sci 49:1597–1615

Tremblay MJ, Loder JW, Werner FE, Naimie CE, Page FH, Sinclair MM (1994) Drift of sea scallop larvae *Placopecten magellanicus* on Georges Banks: a model study of the roles of mean advection, larval behavior and larval origin. Deep-Sea Res II 41:7–49

Visser AW (1997) Using random walk models to simulate the vertical distribution of particles in a turbulent water column. Mar Ecol Prog Ser 158:275–281

Xue H, Incze L, Xu D, Wolff N, Pettigrew N (2008) Connectivity of lobster populations in the coastal Gulf of Maine Part I: Circulation and larval transport potential. Ecol Modell 210:193–211

Zimmerman JTF (1979) On the Euler–Lagrange transformation and the Stokes' drift in the presence of oscillatory and residual currents. Deep-Sea Res I 26:505–520

Editorial responsibility: Alejandro Gallego, Aberdeen, UK

Submitted: December 27, 2013; Accepted: July 30, 2014
Proofs received from author(s): November 14, 2014